Mugla Journal of Science and Technology

RECONSTRUCTION AND ANALYSIS OF JET FLOW BY DYNAMIC MODE DECOMPOSITION

Mustafa Hicret YAMAN*, Department of Mathematics, Faculty of Science, Mugla Sitki Kocman University, Turkiye, mhicretyaman@mu.edu.tr
(https://orcid.org/0000-0001-6483-0140)
Gamze YUKSEL, Department of Mathematics, Faculty of Science, Mugla Sitki Kocman University, Turkiye, ngamze@mu.edu.tr
(https://orcid.org/0000-0003-3578-2762)
Received: 21.03.2023, Accepted: 01.08.2023 | Research Article
*Corresponding author | DOI: 10.22531/muglajsci.1268109

Abstract

In this study, the behavior of Turbulent Jet flow was investigated using Dynamic Mode Decomposition, which is a data-driven, dimension reduction method. Jet flow, which is an important and popular research topic in Fluid Dynamics and engineering applications, was considered as the fluid flow. A Large Eddy Simulation (LES) was performed using the openFOAM software to model the Jet flow. 180 snapshots were generated with the simulation to create a Jet Flow dataset of approximately 150 gigabytes. Firstly, the dynamic modes of the jet flow were extracted from this dataset to reveal the characteristic features of the flow. Then, state estimation for reconstruction of the flow were made. This significantly reduced the CPU and RAM requirement for processing data set and saved lots of disk space for storage. Performance measurements were made for the reconstructed images obtained as a result of the analyses. Two metrics were used for the measurements, namely Root Mean Square Error and Structural Similarity Index.
Keywords: Dynamic Mode Decomposition, Reduced Order Model, Jet Flow, Image Processing, Machine Learning

DiNAMiK MOD AYRIŞIMI İLE JET AKIŞININ YENİDEN OLUŞTURULMASI VE ANALİZİ

Özet

Bu çalışmada, tamamen veri odaklı bir boyut indirgeme metodu olan Dinamik Mod Ayrışımı ile bir akışkanın davranışı incelenmiştir. Akış olarak, Akışkanlar Dinamiğinin ve mühendislik uygulamalarının önemli ve popüler araştırma konularından biri olan türbülanslı Jet Akışı ele alınmıştır. Akışın modellenmesi için gerekli simülasyon openFOAM yazılımı ile gerçekleştirilmiştir. Oluşturulan simülasyon ile 180 adet snapshot üretilerek akışa dair yaklaşık 150 gigabyte'lık veriseti oluşturulmuştur. Bu veriseti ile öncelikle Jet Akışının dinamik modları çıkarılarak akışın karakteristik özellikleri ortaya çıkarılmış, daha sonra akış görüntülerine dair durum tahmini ile akış yeniden oluşturulmuştur. Böylece verisetinin işlenmesi için gereken CPU ve RAM kullanımı önemli ölçüde azalmış, ayrıca sonraki işlemler için saklanacak veriye dair disk depolama alanında ciddi kazanımlar elde edilmiştir. Yapılan analizler sonucunda elde edilen yeniden oluşturulan görüntülerinin performans ölçümleri yapılmıştır. Ölçümler için iki metrik kullanılmış olup bunlar Kök Ortalama Kare Hatası ve Yapısal Benzerlik İndeksi'dir.
Anahtar Kelimeler: Dinamik Mod Ayrışımı, Model Boyut İndirgeme (ROM), Jet Akış, Görüntü İşleme, Makine Öğrenmesi

Cite

Yaman, M. H., Yuksel, G., (2023). "Reconstruction and Analysis of Jet Flow by Dynamic Mode Decomposition", Mugla Journal of Science and Technology, 9(2), 19-24.

1. Introduction

Dynamic Mode Decomposition (DMD) is a powerful data-driven method for analyzing complex and high-dimensional systems. It is a mathematical technique that extracts the underlying spatio-temporal patterns from data generated by dynamical systems.

Schmid and Sesterhenn [1] and Schmid [2] introduced the DMD algorithm in their study and revealed its ability to provide analyses and estimations from high-dimensional fluid data. DMD is an equation-free, data-driven method that can decompose a complex system into spatio-temporal coherent structures that can be used for reconstruction, state estimation and control. In studies that may be fundamental in DMD theory; Mezi'c et al. [3,4,5] and Rowley et al. [6] showed that DMD is linked to underlying nonlinear dynamics through Koopman operator theory [7] and can be easily interpreted using standard dynamical system techniques. DMD can be considered as the perfect fusion of spatial dimensionality reduction methods like proper orthogonal decomposition (POD) and Fourier transforms [8]. The common method for calculating POD is singular value decomposition (SVD) which it can alternatively be described as principal component analysis (PCA) [9,10].

DMD provides an efficient way to identify the dominant modes of variability in a system, enabling researchers to understand the system's behavior and reconstruct the flow to estimate state evolution. DMD has been applied in a wide range of fields, including fluid dynamics, neuroscience, climate science, and finance, among others [8]. Its ability to handle noisy and incomplete data makes it particularly useful in real-world applications.

In this study, DMD is applied to a flow data called Jet Flow. Jet flow analysis is a fundamental problem in fluid dynamics and has important practical applications in fields such as aerospace, energy, and transportation via LES [11,12,13]. Jet flow analysis typically involves the study of various parameters, such as the jet velocity, viscosity of fluid, and nozzle geometry, which can affect the flow behavior. Jet flow can exhibit complex flow phenomena such as turbulence, mixing, and vortex shedding, which can significantly impact the performance of the system.

DMD was used to analyze and estimate the behavior of jet flows. DMD can identify the dominant modes of variability in the jet flow and reconstruct the original data. This makes DMD a powerful tool for understanding the dynamics of jet flows and predicting their behavior under different conditions.

2. Methodology

2.1. Dynamic Mode Decomposition

DMD is a technique for extracting fundamentally coherent structures from data. It can be viewed as the perfect fusion of spatial Proper orthogonal decomposition (POD) and Fourier transformations. For the nonlinear dynamic system that produces the data, DMD builds the most suitable linear dynamic system [14].

An ordinary differential equation, separate from the system's governing equation, is used in the procedure to determine the time evolution of the variable being investigated in the dynamic system;

$$\frac{d\boldsymbol{x}}{dt} = f(\boldsymbol{x}, t; \mu) \tag{1}$$

the dynamics are represented by f, the parameters are represented by μ, and the position of the dynamic system at time t is represented by the vector $\boldsymbol{x}(t)$.

The dynamic system represented by equation (1) in continuous form has the following discrete form:

$$\boldsymbol{x}_{k+1} = F(\boldsymbol{x}_k) \tag{2}$$

Equation (1) can be represented as a linear ordinary differential equation in the DMD method as shown below:

$$\frac{d\boldsymbol{x}}{dt} = \mathbf{A}\boldsymbol{x} \tag{3}$$

here, $x(0)$ is the initial condition. The solution of the equation is given below;

$$\boldsymbol{x}(t) = \sum_{k=1}^{n} \phi_k e^{\omega_k t} b_k = \boldsymbol{\Phi} e^{\boldsymbol{\Omega} t} \boldsymbol{b} \tag{4}$$

here, the coordinates of $x(0)$ based on the eigenvectors are given by $\boldsymbol{b}_k$, while the eigenvalues of the matrix A and their corresponding eigenvectors are denoted by $\boldsymbol{\omega}_k$ and $\boldsymbol{\phi}_k$, respectively.

2.2. DMD Algorithm

Then, the dataset is divided into two parts and separated from one another by a sampling time step Δt, so that

$$\boldsymbol{X} = \begin{bmatrix} \vdots & \vdots & & \vdots \\ \boldsymbol{x}_1 & \boldsymbol{x}_2 & \cdots & \boldsymbol{x}_{m-1} \\ \vdots & \vdots & & \vdots \end{bmatrix} \tag{5}$$

$$\boldsymbol{X}' = \begin{bmatrix} \vdots & \vdots & & \vdots \\ \boldsymbol{x}_2 & \boldsymbol{x}_3 & \cdots & \boldsymbol{x}_m \\ \vdots & \vdots & & \vdots \end{bmatrix} \tag{6}$$

where $\boldsymbol{x}_k \in \mathbb{C}^n (k = 1, \ldots, m)$ is the k th snapshot of the flow field, m is the number of snapshots [2,8].

Assumed to be a linear mapping between $\boldsymbol{X}'$ and $\boldsymbol{X}$

$$\boldsymbol{X}' \approx \boldsymbol{A}\boldsymbol{X} \tag{7}$$

where A is a best-fit linear operator.

In a linear system, calculating A is cheap, but in a nonlinear system, explicitly computing A can be quite expensive, especially when dealing with large dataset. Because of this, the singular value decomposition (SVD) is used once the similarity matrix has been produced.

$$\boldsymbol{A} = \boldsymbol{X}'\boldsymbol{X}^{+} \tag{8}$$

where + is the Moore-Penrose pseudoinverse.

The large state size (n) makes it difficult to analyze matrix A directly in practice; therefore, the SVD is used; instead of decomposing matrix A, the low rank $\tilde{A}$ projected with proper orthogonal decomposition is calculated.

$$\boldsymbol{X} \approx \boldsymbol{U}\boldsymbol{\Sigma}\boldsymbol{V}^* \tag{9}$$

* represents conjugate transpose, $\boldsymbol{U} \in \mathbb{C}^{nxr}, \boldsymbol{\Sigma} \in \mathbb{C}^{rxr}, \boldsymbol{V} \in \mathbb{C}^{mxr}$ and the value r denotes the r -truncation SVD's rank. $\boldsymbol{U}$ and $\boldsymbol{V}$ are both orthogonal, and the $\boldsymbol{\Sigma}$ matrix is diagonal.

As well, A matrix is shown as below

$$\mathbf{A} = \boldsymbol{X}'\mathbf{V}\boldsymbol{\Sigma}^{-1}\boldsymbol{U}^* \tag{10}$$

Then, to replace the full order matrix A, projected matrix $\tilde{A}$ can be constructed by minimizing the Frobenius Norm

$$\|\boldsymbol{X}' - \boldsymbol{A}\boldsymbol{X}\|_F \tag{11}$$

which is

$$\|\boldsymbol{X}\|_F = \sqrt{\sum_{j=1}^{n}\sum_{k=1}^{m} \boldsymbol{X}_{jk}^2} \tag{12}$$

Then A matrix can be obtained by $\tilde{A}$

$$\tilde{\boldsymbol{A}} = \boldsymbol{U}^*\boldsymbol{A}\boldsymbol{U} = \boldsymbol{U}^*\boldsymbol{X}'\mathbf{V}\boldsymbol{\Sigma}^{-1} \tag{13}$$

$$\boldsymbol{A} = \boldsymbol{X}'\mathbf{V}\boldsymbol{\Sigma}^{-1}\boldsymbol{U}^* \tag{14}$$

Next, eigendecomposition of A can be computed so that

$$\boldsymbol{A}\boldsymbol{W} = \boldsymbol{W}\boldsymbol{\Lambda} \tag{15}$$

where the diagonal matrix $\boldsymbol{\Lambda}$ consisting of the $\boldsymbol{W}$ eigenvectors and λ_k eigenvalues. The DMD modes can be achieved via

$$\boldsymbol{\Phi} = \boldsymbol{X}'\mathbf{V}\boldsymbol{\Sigma}^{-1}\boldsymbol{W} \tag{16}$$

3. Numerical Model and Performance Metrics

A jet is a stream of fluid that is ejected into the environment, typically from a nozzle, aperture, or opening of some sort. The jet fluid possesses higher momentum compared to the surrounding environment. In this study, a jet flow system was modeled using a fluid released with high momentum from a square aperture. The model was created in three dimensions by open-source software openFOAM which is popular in CFD and reduced to two dimensions. A total of 180 snapshots were collected from the generated simulation, thus forming the dataset. Details about the fluid and the domain are provided below.

In Figure 1, the 3-dimensional diagram of the geometry in which the flow system will be formed is given. The square opening through which the fluid inlet can be seen on the left. Figure 2 shows a sample flow moment and the mesh grid of the domain. Since this study is handled in two dimensions, the 2D final versions of the mesh and a sample flow snapshot are given in Figure 3 and Figure 4, respectively. In addition, the details of the fluid and simulation are given after Figure 4.

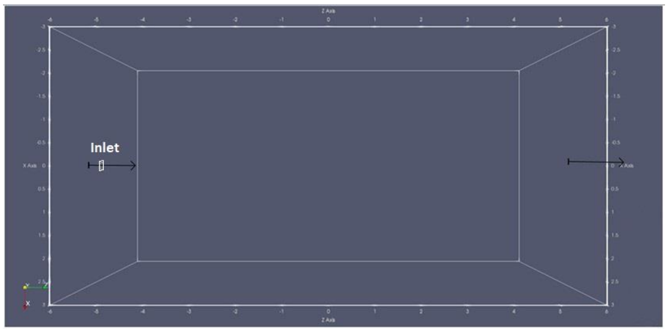

Figure 1. 3D Geometry of LES system.

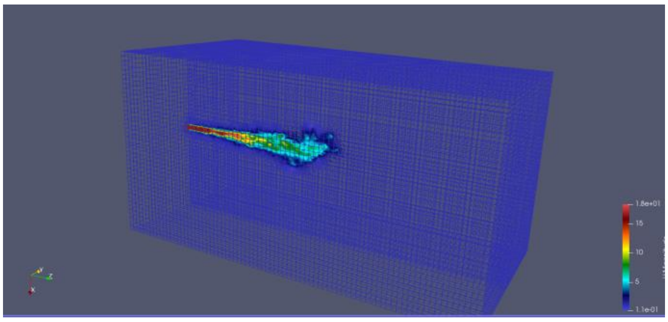

Figure 2. Flow and Domain (3D)

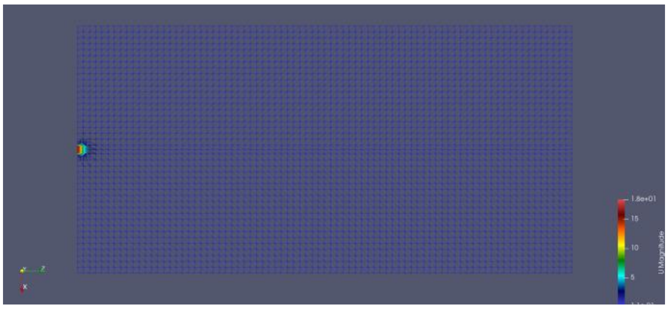

Figure 3. Domain of system (2D).

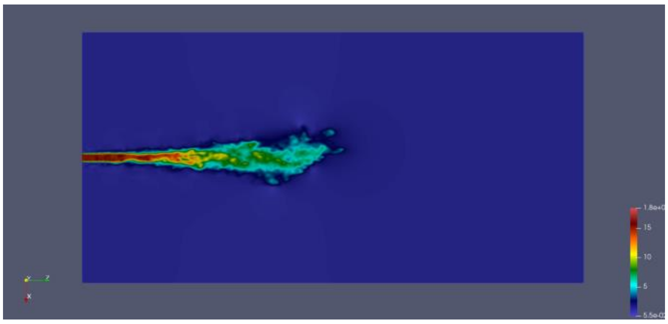

Figure 4. A snapshot of Jet Flow, LES.

The details of the LES flow model are as follows.
Inlet velocity $u = 15\ \frac{m}{s}$, no slip condition at walls and Kinematic Viscosity $\nu = 1.5 \times 10^{-5}\ \frac{m^2}{s}$.
The pimpleFoam algorithm, which is one of the solvers used for vortex flows in the OpenFOAM software, was utilized.
The algorithm solves the continuity equation:

$$\nabla \cdot \boldsymbol{u} = 0 \tag{17}$$

and the momentum equation:

$$\frac{\partial \boldsymbol{u}}{\partial t} + \nabla \cdot (\boldsymbol{u} \otimes \boldsymbol{u}) - \nabla \cdot R = -\nabla p \tag{18}$$

where u is velocity, p is kinematic pressure, R is Stress tensor.

3.1. Performance Metrics

Two metrics were used to measure the performance of the reconstructed images for the current state and the predicted images for the future state obtained from DMD. The first of these metrics is the Structural Similarity Index (SSIM).

The degree of similarity between two given images is determined using the SSIM metric. The three key elements that the Structural Similarity Index measure extracts from an image are Luminance, Contrast, and Structure. The comparison between the two images is built around these three factors. Schema of SSIM is given by Figure 5.

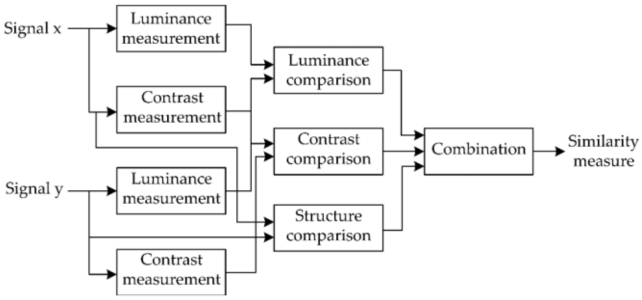

Figure 5. Schema of SSIM

And the following definition of the formula for the SSIM between a test signal y and a reference signal x as follows

$$SSIM(x,y) = [l(x,y)]^{\alpha}[c(x,y)]^{\beta}[s(x,y)]^{\gamma} \tag{19}$$

where $l(x,y)$ denotes the luminance, $c(x,y)$ denotes the contrast and $s(x,y)$ is the structure component. The parameters α , β , $\gamma > 0$ denote a weighted combination of the aforementioned components [15,16,17].

The second metric is called the root mean square error (RMSE), and it measures how much the original and reconstructed images differ from one another. The lower the RMSE value, the more accurate the model is.

$$\sqrt{\frac{\sum_{i=1}^{M}\sum_{j=1}^{N}|R(i,j)-O(i,j)|^2}{M \times N}} \qquad (20)$$

where M and N are size of the image, i and j are the pixel coordinates in the image. R(i,j) is the reconstructed (or predicted) image and O(i,j) is the original image.

4. Result and Discussion

DMD was applied to the dataset created from the snapshots generated by the Jet flow simulation in openFOAM. As a result of DMD, the dominant modes of the flow were selected so the model was reduced, enabling the reconstruction of Jet flow images.

The original images and the reconstructed images for the specified time steps are presented below. In order to compare the performance of the reconstructed images, RMSE, SSIM and PSNR values were calculated for each instantaneous image and the values are presented below.

In Figure 6a and 6b, for the 180th snapshot, it can be observed that the original image and the reconstructed image are almost identical.

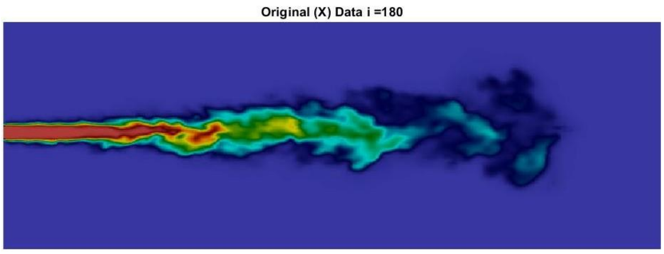

Figure 6a. Original image for 180th snapshot

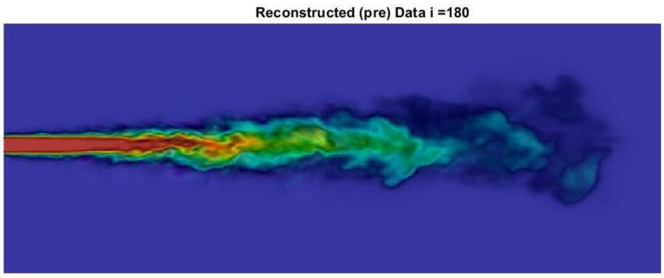

Figure 6b. Reconstructed image for 180th snapshot

In Figure 7, differences between the reconstructed image and the original image are shown separately via RGB channels. The original, the reconstructed, and pixel-based difference images between the two images are given from left to right, respectively, for the red color channel in the first line, the green color channel in the second line, and the blue color channel in the third line.

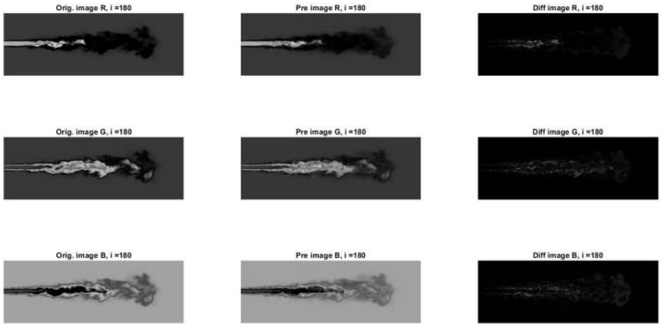

Figure 7. RGB channels of Orig. and Reconst. Image

In addition, the performance metrics of the reconstructed image are given in Table 1.;

Table 1. Performance of reconstruction

$180^{th} snapshot$	
RMSE Value	0,036
SSIM Value	0,987

When the performance metrics are examined; If the RMSE value approaches 0 and the SSIM value approaches 1, that means the two images are almost identical. Looking at the rmse and ssim values calculated for the 180th snapshot, it can be seen that the performance of the reconstructed image is quite good compared to the original.

To see the complete reconstruction performance of the model for each of the 180 snapshots; The RMSE and SSIM values corresponding to each snapshot reconstruction are given in Figure 8.-9. respectively, as follows.

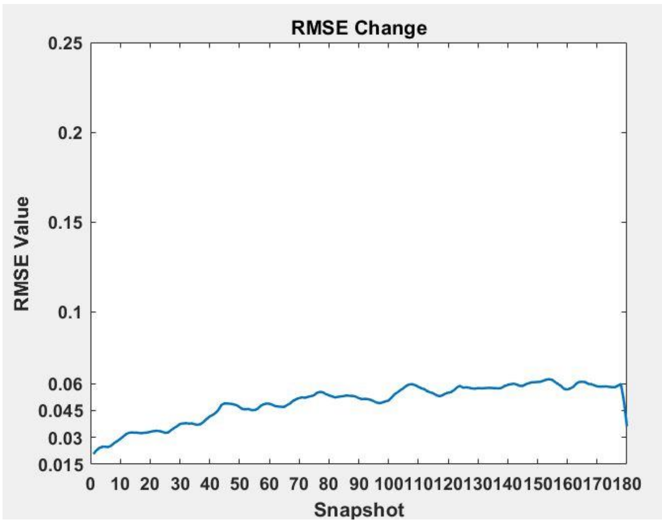

Figure 8. RMSE graph

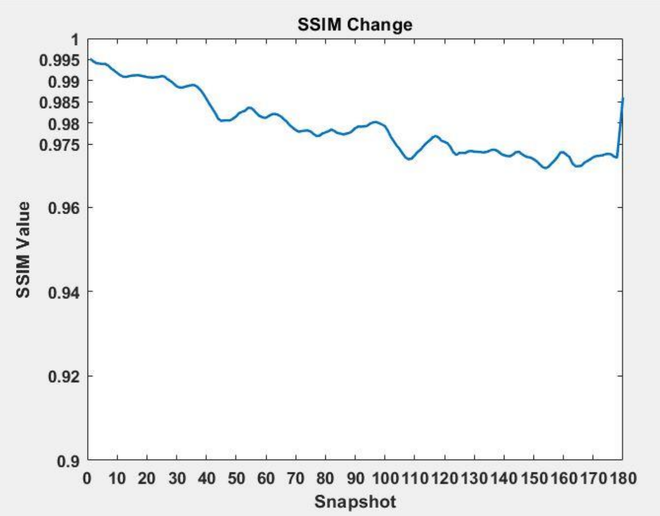

Figure 9. SSIM graph

As can be seen from the graphs given in Figure 8-9., the RMSE of the model has a maximum value of 0,062 and a minimum value of 0,021. The maximum value for the SSIM is 0,998 and the minimum is 0,971.

In addition to these analyzes, the reconstruction of the 180th snapshot was evaluated according to the reduced order model. In Figure 10a.-10f., original image, reconstructed image by truncated 120 modes, truncated 90 modes, truncated 30 modes, and the reconstructed image by truncated 10 modes of 180th snapshot, respectively, are given below.

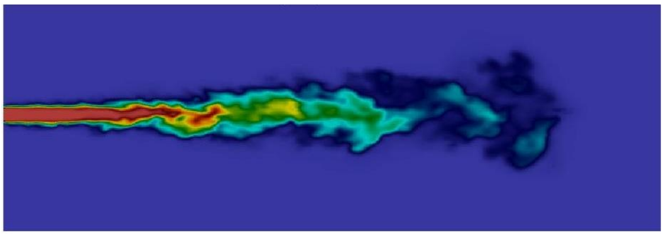

Figure 10a. original image

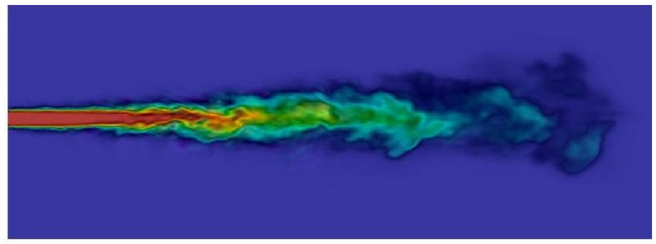

Figure 10b. r=120 modes

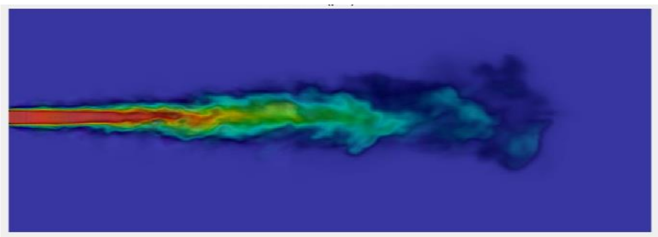

Figure 10c. r=90 modes

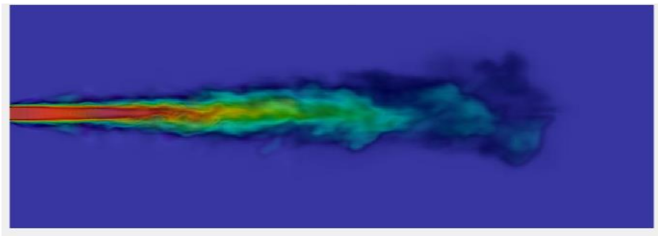

Figure 10d. r=60 modes

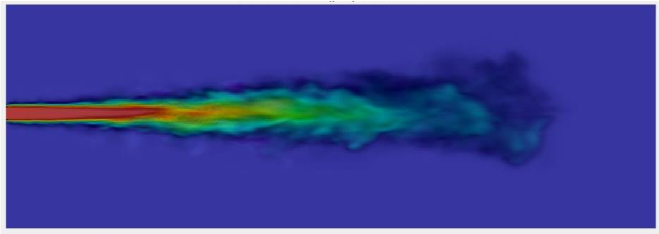

Figure 10e. r=30 modes

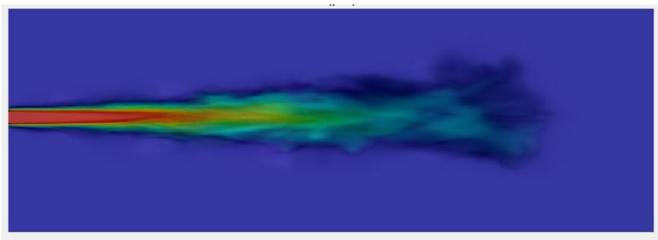

Figure 10f. r=10 modes

The performance metric values of the reconstructed flow images given above and produced by the reduced order model are given below in Table 2.

Table 2. Performance of reduced order model by modes

$180^{th}snapshot$		
truncate rank r	RMSE Value	SSIM Value
r=120	0,036	0,987
r=90	0,039	0,982
r=60	0,047	0,976
r=30	0,052	0,962
r=10	0,066	0,943

When the performance values of the reduced model are examined, it can be seen that the flow created by the r-120 model is almost identical to the original flow. Similarly, the r-90 and r-60 also captured the flow characteristic accurately, even in nonlinear regions and where eddies are intense. These results are supported by SSIM and RMSE metrics in Table 2.

When the r-30 and r-10 are examined, more DMD modes should be included to improve the reconstruction performance, especially in nonlinear and eddy regions, yet more laminar flow models without large vortexes, the flow can be captured accurately by choosing a much smaller number of DMD modes.

In addition to all these processes, one of the most important purposes of reduced order DMD is to reduce the cost of computations needed to process data and the storage cost of the data needed required for post-processing. On the other hand, it can be difficult to post-process this large dataset because of its high CPU and Memory occupancy. However, while reduced order DMD models preserve the details of the original flow, they also provided significant calculation and storage savings. Such as in the current study, the r-120 model reduced data size by 1.5 times, r-90 by 2 times, r-60 by 3 times, r-30 by 6 times, and r-10 by 18 times. Details about disk space saving were given in Table 3.

Table 3. Disk space Economy

truncate rank r	Data Size Reduction (Disk Space Economy %)
r=120	%33,3
r=90	%50
r=60	%66,6
r=30	%83,3
r=10	%94,45

Thus, the CPU and RAM requirement for data processing has been significantly reduced. More importantly, the DMD model does not require any original data to be stored for post-processing, thus saving lots of gigabytes of disk space.

5. Acknowledgement

This study is produced from the first author's dissertation as titled "Dynamic Mode Decomposition of Fluid Flows".

6. References

[1] Schmid, P. J. and Sesterhenn, J., "Dynamic mode decomposition of numerical and experimental data", *In 61st Annual Meeting of the APS Division of Fluid Dynamics. American Physical Society*, 2008.
[2] Schmid, P. J., "Dynamic mode decomposition of numerical and experimental data", *Journal of Fluid Mechanics*, 656, 5–28, 2010.
[3] Mezi´c, I., and Banaszuk, A., "Comparison of systems with complex behavior", *Physica D: Nonlinear Phenomena*, 197, 101–133,2004.
[4] Mezi´c, ı., "Spectral properties of dynamical systems, model reduction and decompositions", *Nonlinear Dynamics*, 41, 309–325, 2005.
[5] Mezi´c, I., "Analysis of fluid flows via spectral properties of the Koopman operator", *Annual Review of Fluid Mechanics*, 45, 357–378, 2013.
[6] Rowley, C. W., Mezi´c, I., Bagheri, S., Schlatter, P. and Henningson, D. S., "Spectral analysis of nonlinear flows", *Journal of Fluid Mechanics*, 645, 115–127, 2009.
[7] Koopman, B. O., "Hamiltonian systems and transformation in Hilbert space", *Proceedings of the National Academy of Sciences of the USA*, 17, 315–318, 1931.
[8] Kutz, J. N., Brunton, S. L., Brunton, J. L., Proctor, J. L., *Dynamic Mode Decomposition: DataDriven Modeling of Complex Systems*, SIAM, 2016
[9] Pearson, K., "On lines and planes of closest fit to systems of points in space", *Philosophical Magazine*, 2, 559–572, 1901.
[10] Jolliffe, I., "Principal Component Analysis", *Encyclopedia of Statistics in Behavioral Science*, 3, 1580–1584, 2005.
[11] Vuorinen, V., Wehrfritz, A, Yu, J., Kaario, O., Larmi, M. and Boersma, B "Large-eddy simulation of subsonic jets," *Journal of Physics: Conference Series*, 318, 32-52, 2011.
[12] Freund, J. and Colonius, T., "Turbulence and sound-field pod analysis of a turbulent jet," *International Journal of Aeroacoustics*, 8-4, 337-354, 2009.
[13] Meyer, K., Pedersen, J. and Ozcan, O., "A turbulent jet in crossflow analysed with proper orthogonal decomposition," *Journal of Fluid Mechanics*, 583, 199-228, 2007.
[14] Tu, J. H., Rowley, C. W., Luchtenburg, D. M., Brunton, S. L. and Kutz, J. N., "On dynamic mode decomposition: Theory and applications", *Journal of Computational Dynamics*, 1(2), pp. 391–421, 2014.
[15] Sevcik, L., Voznak, M., Frnda, J., "QoE Prediction Model for Multimedia Services in IP Network, Applying Queuing Policy", *17th International Symposium on Performance Evaluation of Computer and Telecommunication Systems (SPECTS) part of Summer Sim Multi conference*, 2014, 593-598.
[16] Frnda, J., Nedoma, J., Vanus, J., Martinek, R., A Hybrid "QoS-QoE Estimation System for IPTV Service", *Electronics*,8, 585, 2019.
[17] Frnda, J., Durica, M., Savrasovs, M., "Fournier-Viger, P. and Lin, J., QoS to QoE Mapping Function for Iptv Quality Assessement Based on Kohonen Map: A Pilot Study", *Transport and Telecommunication Journal*,21, 181-190, 2020.